International Journal of Thermophysics, Vol. 25, No. 6, November 2004 (© 2004)

3-D Simulations of Diffusivity Measurements in Liquids with an Applied Magnetic Field

Y. Y. Khine[1] and R. M. Banish[2,3]

Received June 7, 2004

The effect of convective contamination in self-diffusivity experiments of liquid metals is predicted via a three-dimensional (3-D) model that includes an applied magnetic field. A uniform heat flux is applied at the sidewall of the cylindrical ampoule, and heat losses are allowed at the top and bottom walls of the ampoule. A wide range of a uniform, steady, axial magnetic field (from moderate to very strong) is considered in the model. Since the thermal Péclet number, Pe, is very small for the parameters of interest, convective heat transfer is neglected. A large interaction parameter, N, suggests that the flow is inertialess. The temperature and flow problems are solved at steady state while the time-dependent concentration problem is determined for various mass Péclet numbers, Pe_{m}. In all cases, the output D (i.e., with convective contamination) increases with an increase in the temperature non-uniformity ΔT_θ. The radial and azimuthal velocities are much smaller than the axial velocity in each case. A stronger magnetic field can tolerate a higher temperature non-uniformity ΔT_θ, but ΔT_θ is still less than 0.025 K with a 5 T magnetic field for convective contaminations to be less than 5% of the total mass flux.

KEY WORDS: convective contamination; liquid metals; magnetic field; three-dimensional mass diffusion.

1. INTRODUCTION

The presence of natural or buoyant convection due to temperature non-uniformities under gravity (or maybe even in microgravity) is undesirable

[1]Center for Materials Research, University of Alabama in Huntsville, Huntsville, Alabama 35899, U.S.A.
[2]Center for Materials Research and Department of Chemical and Materials Engineering, University of Alabama in Huntsville, Huntsville, Alabama 35899, U.S.A.
[3]To whom correspondence should be addressed. Email: banishm@uah.edu.

0195-928X/04/1100-1763/0

in diffusivity measurements of liquids as it may enhance the mass transfer. Since accurate measurements are very important for further applications in materials processing, it is essential to suppress the convection in the liquids. Due to large electrical conductivities of liquid metals and semiconductors, researchers have applied magnetic fields in order to suppress the convection in the experiments. Our first self-diffusivity model that represented the experiment in the presence of a steady, uniform magnetic field was determined for a 2-D axisymmetric case, and the results were published for a moderate to strong magnetic field with various heating conditions [1,2]. The numerical results suggested that the application of a strong magnetic field leads to higher "allowable" temperature nonuniformities in the liquid but in the presence of a nonuniform, steady heat transfer condition in order to obtain acceptable results.

Alexander et al. [3] studied a 3-D time-dependent diffusivity model in the presence of terrestrial gravity. They found that for horizontal temperature non-uniformities across the sample as small as 0.1 and 1 K, the convective transport rates exceed the diffusive transport rates in 1 and 3 mm diameter capillaries. This paper is a continuation of the previous work by Alexander et al. [3] in the presence of an applied magnetic field. This is the first 3-D numerical model, and a steady, uniform heating condition is imposed to the model for a wide range of steady magnetic field strength. While the radial temperature nonuniformity is the driving force of buoyant convection in the previous, 2-D axisymmetric model, an azimuthal variation in temperature is considered in addition to the radial temperature gradient in the 3-D model. Steady-state thermal and flow problems are determined given that the applied heat flux is steady during the measurements. Then, the time-dependent mass diffusion problem is solved with the known thermal and flow solutions. The simulated results for a moderate to strong applied magnetic field are presented in this paper.

2. PROBLEM FORMULATION

The model fluid is assumed to be a Boussinesq fluid, and is enclosed within a vertical cylinder of 3 mm diameter and 30 mm in height. The gravitational acceleration g acts downward along the vertical axis of the cylinder, and the steady, uniform magnetic field B is applied in the opposite direction. A steady, uniform heat flux is applied through the sidewall of the cylinder during the measurements. The isopycnic radioactive tracer is placed at one end of the cylinder at the beginning of the measurements. A radiation shield with two bores is placed parallel to the vertical axis where the amount of tracer is measured which is directly proportional to the concentration at those two locations. The origin is placed at the center

of the bottom wall of the cylinder so that the sidewall lies at $r=1$, the bottom wall is at $z=0$, and the top wall is at $z=b$ which is 20 using the radius R as the characteristic length.

In this 3-D model, the characteristic velocity to non-dimensionalize the dimensional velocities is defined as $U=\rho g\beta\Delta T_\theta/(\sigma B^2)$, where ρ is the uniform density of the fluid, β the volumetric expansion coefficient for Boussinesq approximation, ΔT_θ the maximum horizontal temperature difference across the cylinder at any height z, and σ is the electrical conductivity of the fluid. For a moderate to strong applied magnetic field, the characteristic velocity U is small enough that the thermal Péclet number $Pe=\rho c_{\mathrm{h}}UR/\lambda$ becomes very small; usually <1. Here, c_{h} is the specific heat and λ is the thermal conductivity of the fluid. Under this condition, the convective heat transfer is assumed negligible and the time-independent energy equation ($\nabla^2 T=0$) is non-dimensionalized by R for length and ΔT_θ for temperature. The boundary conditions for the thermal problem are: $T(1,\theta,z)=0.5(1+\cos\theta)+(\Delta T_z/\Delta T_\theta)\,(z/b)$ at the sidewall, where ΔT_z is the temperature difference between the top and bottom wall of the cylinder; $T(r,\theta,0)=0.5(1+r\cos\theta)$ at the bottom wall; and $T(r,\theta,b)=0.5(1+r\cos\theta)+(\Delta T_z/\Delta T_\theta)$ at the top wall of the cylinder. The analytical solution for the thermal problem with given boundary conditions is

$$T(r,\theta,z)=0.5(1+r\cos\theta)+\left(\frac{\Delta T_z}{\Delta T_\theta}\right)\left(\frac{z}{b}\right). \tag{1}$$

Once the temperature solution is obtained, the flow problem is determined. The characteristic ratio of the electromagnetic body force to the inertial effect is known as the interaction parameter $N=\sigma B^2 R/(\rho U)$, and this ratio is very large for sufficiently strong magnetic field. Thus, the inertial effect becomes negligible in the Navier–Stokes equations. In addition to the applied magnetic field, the associated currents produce a magnetic field known as an induced magnetic field. The characteristic ratio of the induced applied magnetic fields is the magnetic Reynolds number $R_{\mathrm{m}}=\mu_{\mathrm{p}}\sigma UR$, where μ_{p} is the magnetic permeability of the fluid. This parameter is usually very small for characteristic velocities in diffusivity experiments and the liquids of interest, and thus the induced magnetic field is negligible in the model.

The dimensionless equations for the steady, inertialess flow problem are

$$\nabla\cdot\boldsymbol{v}=0, \tag{2a}$$

$$\nabla p=T\hat{\boldsymbol{z}}+\boldsymbol{j}\times\hat{\boldsymbol{z}}+Ha^{-2}\nabla^2\boldsymbol{v}, \tag{2b}$$

$$\nabla \cdot \boldsymbol{j} = 0, \tag{2c}$$

$$\boldsymbol{j} = -\nabla\phi + \boldsymbol{v} \times \hat{\boldsymbol{z}}. \tag{2d}$$

Equation (2a) ensures the conservation of mass in the fluid. Equation (2b) is the Navier–Stokes equation with a buoyancy force and an electromagnetic body force. Here, the magnetic flux is scaled by B, p is the reduced pressure and normalized by $\sigma U B^2 R$, $\boldsymbol{j}$ is the electric current density normalized by $\sigma U B$, and $Ha = BR(\sigma/\mu)^{1/2}$ is the Hartmann number representing a ratio of electromagnetic effects to viscous effects in the fluid with viscosity μ. Equation (2c) is the continuity of electric current density, and Eq. (2d) is Ohm's law and is made up of the static electric field $\nabla\phi$ and the induced electric field due to the interaction between the melt motion and the applied magnetic field. ϕ is the electric potential function and is scaled by UBR.

No slip boundary condition is applied at the walls of the cylinder. The Chebyshev spectral collocation method is used to solve the flow problem. Collocation points from 22 to 50 are required in the radial direction, while 70–160 collocation points are needed in the axial direction for the range of magnetic fields considered.

Once the flow solution is known, the time-dependent mass diffusion problem is determined. The dimensionless governing equation for the diffusion problem is

$$\frac{\partial c}{\partial t} + Pe_{\mathrm{m}}(\boldsymbol{v} \cdot \nabla)c = \nabla^2 c, \tag{3a}$$

where $Pe_{\mathrm{m}} = UR/D_0$ is the mass Péclet number which is a characteristic ratio of convective effects to diffusive effects in the liquid. In Eq. (3a), c is normalized by the initial concentration C_0 and t is scaled by the diffusion time scale R^2/D_0. The boundary conditions are that no mass transport is allowed across any boundary. The initial condition is that a thin layer of radioactive tracer occupies the bottom of the cylinder at the beginning of the measurements and is represented by

$$c(r, z, t = 0) = \exp(-\gamma z^2), \tag{3b}$$

where $\gamma = 2.5$.

The spectral collocation method is used for the spatial discretization while the finite difference method is used in temporal discretization in solving the diffusion problem. The fluid flow is symmetric about the plane at $\theta = 0$ and $\theta = \pi$, and thus the concentration c is symmetric about this plane. In Chebyshev polynomials, c is defined as

$$c(r, \theta, z, t) = \sum_{M=0}^{N_\theta} \cos(M\theta) C_M(r, z, t), \tag{3c}$$

where cosine is an even function. Then, the time traces of $c(r, \theta, z, t)$ are straight lines fitted with the form,

$$\ln[c_1(t) - c_2(t)] = \text{constant} - \left(\frac{\pi^2 D}{Z^2}\right) t \tag{3d}$$

known as the Codastefano [6] or Harned [7] technique in order to obtain the output D.

3. RESULTS AND DISCUSSION

Liquid indium with the following properties, $\mu = 5.18 \times 10^{-4}\,\text{kg} \cdot \text{m}^{-1} \cdot \text{s}^{-1}$, $\rho = 6.64 \times 10^3\ \text{kg} \cdot \text{m}^{-3}$, $\beta = 1.02 \times 10^{-4}\,\text{K}^{-1}$, and $\sigma = 3.02 \times 10^6\,\text{S} \cdot \text{m}^{-1}$ [4], is used as a model fluid. A self-diffusivity value of $D_0 = 1.48 \times 10^{-5}\,\text{cm}^2 \cdot \text{s}^{-1}$ was used as input. Five different magnetic field strengths from moderate to very strong (i.e., $Ha = 25$–600) are considered for the uniform incoming heat flux along the sidewall during the measurements.

With a uniform heat flux along the sidewall of the cylinder, the contours of the velocities are presented in Figs. 1–3 for $B = 3.49\,\text{T}$ ($Ha = 400$). The magnitude of v_r varies as cos θ in the azimuthal direction, and the

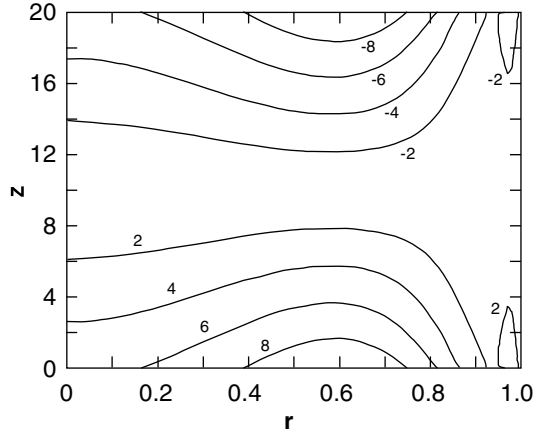

Fig. 1. Contours of radial velocity v_r in $\theta = 0$ plane for $Ha = 400$.

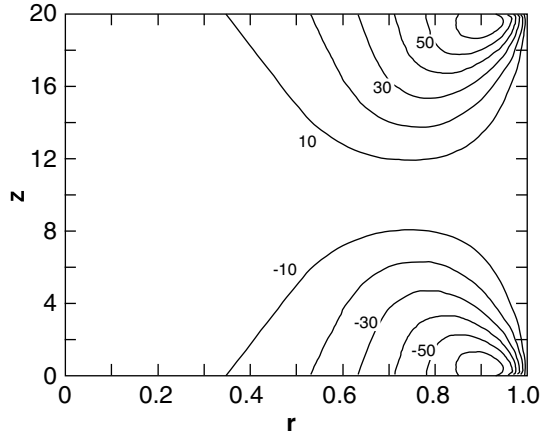

Fig. 2. Contours of azimuthal velocity v_θ in $\theta = 0$ plane for $Ha = 400$.

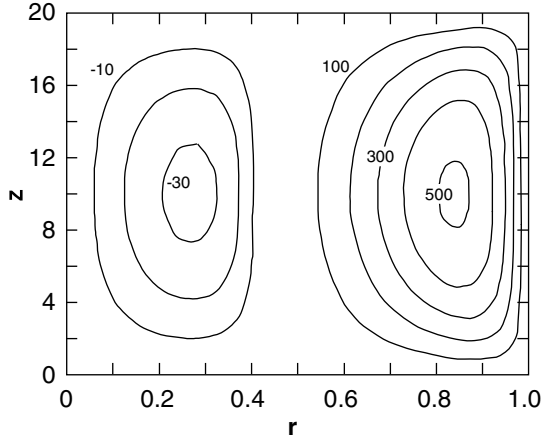

Fig. 3. Contours of axial velocity v_z in $\theta = 0$ plane for $Ha = 400$.

contours of v_r can be seen in Fig. 1 for the $\theta = 0$ plane. They have symmetry at the mid-plane $z = 10$. The contours range from -9.78 to 9.78. For a smaller magnetic field from $B = 3.49$ T, the v_r contours are horizontal toward the centerline ($r = 0$) while with a higher magnetic field, the contours tend to be compressed toward the sidewall ($r = 1$). The v_r contours range in the order of -10 and 10 for all five cases. Ma and Walker [5] presented the asymptotic solutions with a non-axisymmetric temperature in a Czochralski crystal growth process with an axial magnetic field. Their v_r contours for $Ha = 200$ are similar to those in Fig. 1.

The magnitude of v_θ varies as $\sin\theta$ in the azimuthal direction, and the v_θ contours at the $\theta = 0$ plane are presented for $Ha = 400$ in Fig. 2. They are positive near the top wall and negative near the bottom wall. The v_θ contours range between -66.5 and 66.5 and have symmetry at the midplane ($z = 10$). The contours are horizontal toward the centerline for lower Ha with smaller magnitudes. For stronger magnetic fields (higher Ha), the contours are compressed toward the sidewall ($r = 1$) with increasing magnitude with an increase in Ha. These contours are similar in pattern to those presented by Ma and Walker [5] for v_θ with $Ha = 200$ from the asymptotic solution.

The magnitude of v_z varies as $\cos\theta$ in the azimuthal direction, and the v_z contours at the $\theta = 0$ plane are presented in Fig. 3 for $Ha = 400$. The contours are positive near the sidewall ($r = 1$), and a negative weak circulation appears near the centerline for $Ha \geqslant 400$. They are symmetric at the midplane ($z = 10$) and range from -33 to 515. The magnitude of v_z contours increases with increasing Ha, and the contours are compressed toward $r = 1$. Ma and Walker [6] presented v_z contours of this nature from an asymptotic solution for $Ha = 200$.

The allowable temperature nonuniformities ΔT_θ are very small for any Ha in this setup. The absolute maximum radial velocities $|v_{r\max}|$ are in the range of 10^{-5}–$10^{-6}\,\mathrm{cm}\cdot\mathrm{s}^{-1}$ and are the smallest among the three velocity components for all cases. The absolute maximum azimuthal velocities $|v_{\theta\max}|$ are comparable to the $|v_{r\max}|$ for moderate Ha, and they are an order of magnitude higher than $|v_{r\max}|$ for higher Ha. The absolute maximum axial velocities $|v_{z\max}|$ are in the range of 10^{-4}–$10^{-5}\,\mathrm{cm}\cdot\mathrm{s}^{-1}$ and the largest component of the velocity vector. The uniform axial magnetic field suppresses the radial velocities but since they are parallel to the axial velocities, there is no significant effect in reducing the axial velocities. All the velocities increase with increasing ΔT_θ resulting in higher output D. The velocities vary as B^{-2} with the applied uniform axial magnetic field.

A summary of results for our 3-D model can be seen in Table I. In numerical simulations, the results with $N_\theta = 2$ and $N_\theta = 4$ agree up to 12 significant figures and thus, neglecting the higher modes in Chebyshev polynomials of $c(r, \theta, z, t)$ is justifiable. A range of magnetic fields from a moderate field of $B = 0.218\,\mathrm{T}$ ($Ha = 25$) to a very strong field of $B = 5.24\,\mathrm{T}$ ($Ha = 600$) is considered for this 3-D model. The maximum absolute values of the three components of the velocity vector are presented for each case along with the output D. For the same magnetic field, the velocities depend directly on the allowable temperature non-uniformity ΔT_θ in the liquid; however, the output D is not proportional to the temperature and flow results. For example, an increase of ΔT_θ by a factor of two does not

Table I. Summary of Results

ΔT_θ(K)	$\lvert v_{r\,\max}\rvert$ (cm · s^{-1})	$\lvert v_{\theta\,\max}\rvert$(cm · s^{-1})	$\lvert v_{z\,\max}\rvert$ (cm · s^{-1})	$D\times10^5$ (cm^2 · s^{-1})
$B=0.218$ T; $Ha=25$				
0.000853	1.04×10^{-5}	1.04×10^{-5}	5.90×10^{-5}	1.51
0.00149	1.81×10^{-5}	1.81×10^{-5}	1.03×10^{-4}	1.58
0.00213	2.59×10^{-5}	2.59×10^{-5}	1.47×10^{-4}	1.69
0.00639	7.76×10^{-5}	7.76×10^{-5}	4.42×10^{-4}	3.31
$B=0.873$ T; $Ha=100$				
0.00137	3.83×10^{-6}	5.20×10^{-6}	5.40×10^{-5}	1.51
0.00273	7.64×10^{-6}	1.04×10^{-5}	1.08×10^{-4}	1.58
0.00410	1.15×10^{-5}	1.56×10^{-5}	1.62×10^{-4}	1.71
0.0137	3.83×10^{-5}	5.20×10^{-5}	5.40×10^{-4}	3.90
$B=1.75$ T; $Ha=200$				
0.00412	2.86×10^{-6}	8.93×10^{-6}	7.85×10^{-5}	1.53
0.00824	5.71×10^{-6}	1.79×10^{-5}	1.57×10^{-4}	1.67
0.0165	1.14×10^{-5}	3.58×10^{-5}	3.14×10^{-4}	2.23
$B=3.49$ T; $Ha=400$				
0.00819	1.45×10^{-6}	9.85×10^{-6}	7.62×10^{-5}	1.51
0.0164	2.90×10^{-6}	1.97×10^{-5}	1.52×10^{-4}	1.60
0.0328	5.80×10^{-6}	3.40×10^{-5}	3.04×10^{-4}	1.96
$B=5.24$ T; $Ha=600$				
0.0123	1.05×10^{-6}	1.04×10^{-5}	7.53×10^{-5}	1.50
0.0246	2.10×10^{-6}	2.07×10^{-5}	1.50×10^{-4}	1.57
0.0492	4.20×10^{-6}	4.16×10^{-5}	3.01×10^{-4}	1.83

result in a factor of two increase in the output D with the same magnetic field, but the components of the velocity vector are a factor of two larger.

Figure 4 presents the dependence of output D on the effective mass Péclet number (effective $Pe_{\rm m}$), which is $Pe_{\rm m}\cdot|v_{max}|$, for different magnetic field strengths. The effective $Pe_{\rm m}$ represents the convective mass transport to mass diffusion, and five different magnetic fields are considered. For the $Ha=25$ case, the output D is the most sensitive to the buoyant convection produced by the applied uniform heat flux. As the applied magnetic field is increased, the sensitivity of output D on the convective contamination decreases as one would expect. For example, at an effective $Pe_{\rm m}\sim3$, the output D is 1.3 times larger for $Ha=25$ than that for $Ha=600$ having a comparable magnitude of convective contamination in the measurements. Thus, a stronger magnetic field can tolerate a larger allowable temperature nonuniformity ΔT_θ.

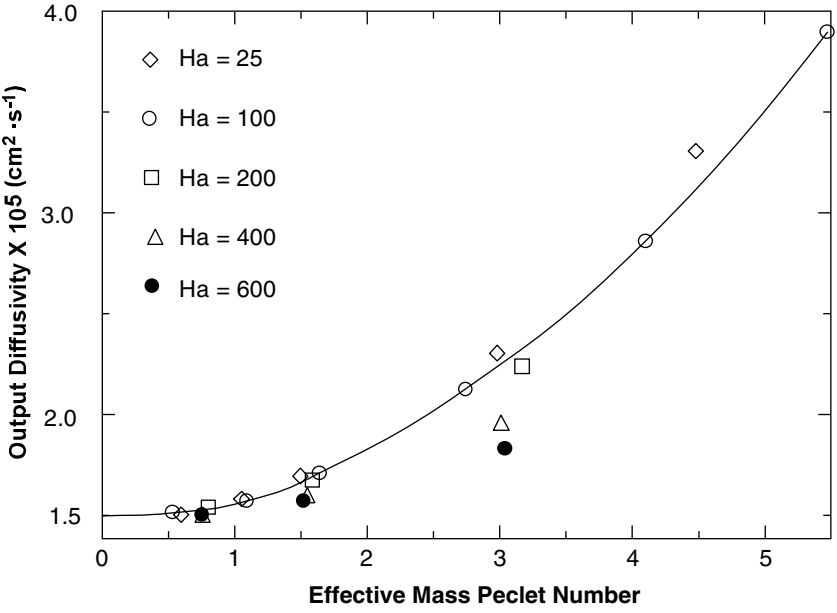

Fig. 4. Output D versus effective mass Péclet number (effective Pe_{m}) for different magnetic field strengths.

From the 3-D numerical simulations by Alexander et al. [3] on liquid indium, for a 3 mm diameter capillary with an allowable temperature nonuniformity $\Delta T_\theta = 0.01$ K, the output D, from considering the entire cross section, is 1.54×10^{-5} cm$^2 \cdot$ s^{-1}. Our results from Table I with a magnetic field of $B = 5.24$ T ($Ha = 600$) gives an output $D = 1.50 \times 10^{-5}$ cm$^2 \cdot$ s^{-1} for an allowable $\Delta T_\theta = 0.0123$ K. Therefore, the application of a strong magnetic field does not have a significant benefit on suppressing the convection in the liquid during the measurements.

4. CONCLUSIONS

A first 3-D numerical model representing a self-diffusion experiment for liquids with an applied magnetic field is presented in this paper. The applied uniform heat flux drives the buoyant convection during the diffusivity measurements, and five different magnetic field strengths are considered. The components of the velocity vector are symmetric at the mid-plane ($z = 10$). Each component of the velocity vector increases with increasing applied heat flux (i.e., allowable temperature nonuniformity ΔT_θ in the liquid) and decreases with increasing applied uniform magnetic field.

The magnitudes of the radial and azimuthal velocities are comparable while the axial velocities are significantly larger than the other two components.

While the components of the velocity vector are directly proportional to the allowable temperature nonuniformity ΔT_θ in any case, the output D does not have a linear relationship with the applied heat flux or ΔT_θ . The output D depends on both the ΔT_θ and the magnitude of the applied magnetic field, and in order to achieve the desired 5% allowable convective contamination in the liquid (i.e., the output D must be $1.55 \times 10^{-5}\,\mathrm{cm}^2 \cdot \mathrm{s}^{-1}$), an optimum heat flux or ΔT_θ can be estimated from the results provided in Table I for different magnetic field strengths. Although a strong magnetic field can tolerate a larger ΔT_θ, the applied axial magnetic field cannot suppress the axial velocities significantly in this setup. The allowable ΔT_θ are extremely small, even for a very strong magnetic field of 5.24 T ($Ha = 600$) case.

In conclusion, there is no notable improvement in applying a uniform, axial magnetic field to the 3-D model created by Alexander et al. [3] although liquid indium is electrically conducting. However, from our previous work on a 2-D axisymmetric model with an applied magnetic field and different forms of heat fluxes [1,2], it was recognized that a particular form of heat transfer is important in bringing out the benefit of a magnetic field. Although the application of a magnetic field does not show significant benefit to the current 3-D model with a uniform heat flux along the sidewall, we believe that it would be beneficial in controlling the buoyant convection in the 3-D model with an appropriate form of heat transfer.

ACKNOWLEDGMENTS

The support by the National Aeronautics and Space Administration through Grants NCC8-99 and NAG8-1476 for this research is gratefully acknowledged. We are thankful to Professor J. S. Walker at University of Illinois at Urbana-Champaign for his guidance and suggestions. We gratefully acknowledge the National Center for Supercomputing Application in Champaign, Illinois and Alabama Supercomputing Center for access to their facilities.

REFERENCES

1. Y. Y. Khine, R. M. Banish, and J. I. D. Alexander, *Int J. Thermophys.* **23**:649 (2002).
2. Y. Y. Khine, R. M. Banish, and J. I. D. Alexander, *J. Crystal Growth* **250**:274 (2003).
3. J. I. D. Alexander, J.-F. Ramus, and F. Rosenberger, *Microgravity Sci Tech.* **9**: 158 (1996).

4. T. Ida and R. I. L. Guthrie, in *The Physical Properties of Liquid Metals* (Clarendon, Oxford, 1988).
5. N. Ma and J. S. Walker, *J. Fluids Eng*. **118**:155 (1996).
6. P. Codastefano, A. Di Russo, and V. Zanza, *Rev. Sci. Instrum*. **48**:1650 (1977).
7. H. S. Harned and R. L. Nuttall, *J. Am. Chem. Soc*. **69**:736 (1947).